

## DISCUSSION

The present study shows the first evidence regarding a tumor-promoting role of EBAG9 *in vivo*. We showed that Renca tumors overexpressing EBAG9 had a much aggressive phenotype with poorer prognosis as compared to Renca tumors expressing empty vector, although the effects of EBAG9 on culture cell proliferation was relatively minimal. EBAG9 immunoreactivity was detected in most of human RCC samples and high amounts of EBAG9 protein may associate with poor prognosis of the patients. Our findings suggest that EBAG9 is a tumor-promoting factor in RCC yet does not function as an essential oncogene by itself. The present results lead us to the notion that EBAG9 potentiates tumor growth by altering tumor microenvironment.

Decreased local immune responses may one of the critical mechanisms that change tumor microenvironment. In antitumor immunity, T lymphocyte-mediated immune surveillance is thought to be a principal host defense mechanism (15). Although tumors such as RCC are immunogenic and could be targeted by tumor-specific CTL or natural killer cells, antitumor immune reactions are not completely effective to reject tumor cells so that tumors continue to grow progressively (16). In our cytotoxicity assay, there was no significant difference of CTL lysis between Renca-EBAG9 and Renca-vector cells, suggesting that overexpression of EBAG9 may not particularly alter the presentation of tumor-associated antigens or the levels of MHC class I molecule expression. In TIL assay, however, CD8<sup>+</sup> T cells seemed to be specifically reduced by aberrant EBAG9 expression. We suspect that generation of immunosuppressive factors or apoptosis activation may result in the reduction of CD8<sup>+</sup> TIL, leading to hamper antitumor immunity.

The alteration in cell surface glycosylation could be implicated in the modulation of tumor microenvironments (17, 18). It has been recently shown that tumor-associated ganglioside expression in human RCC cells suppresses nuclear factor- $\kappa$ B activation in T cells and mediates T-cell apoptosis (19, 20). RCC display increased levels of gangliosides including GM2, GM1, and GD1a (21) as well as several disialogangliosides (22), which may inhibit the function of antigen presenting cells (23) or modulate tumor vascularization (24). It has been recently shown that tumor-associated O-linked glycan antigens Tn and TF were expressed in transfected cells expressing RCAS1 (receptor-binding cancer antigen expressed on SiSo cells)(25), whose cDNA has been found to be a homolog of EBAG9 (26).

Another possible explanation is that EBAG9 may stimulate angiogenesis by up-regulating growth factors or cytokines. There are literatures that vascular endothelial growth factor (VEGF) could be involved in RCC tumor progression. Mutations of the von Hippel-Lindau tumor suppressor gene, which are often observed in hereditary RCC and sporadic clear-cell RCC, result in overproduction of VEGF through a mechanism involving hypoxia-inducible factor  $\alpha$  (27, 28). It has been recently shown that VEGF interferes with the development of T cells at pathologically relevant concentrations *in vivo* (29), thus the growth factor may contribute to tumor-associated immune deficiencies.

It has been generally accepted that tumor cells may escape from immune surveillance by expressing the EBAG9 homolog RCAS1, which targets RCAS1 receptor-expressing immune cells

and induces apoptosis (26). Nakashima *et al.* identified the RCAS1 cDNA through expression cloning using the 22-1-1 monoclonal antibody that they originally generated (30). Engelsberg *et al.* recently showed, however, that the 22-1-1 epitope was distinct from the products encoded by RCAS1 cDNA, because RCAS1 protein was not recognized by the 22-1-1 antibody whereas the 22-1-1 antibody recognized the tumor-associated *O*-linked glycan antigens (25). They showed that their raised polyclonal antibody recognized a ~35 kDa protein, consistent with the immunoblotting results using our polyclonal antibody. On the contrary, putative RCAS1 protein recognized by the 22-1-1 antibody was identified as a ~80-kDa membrane molecule expressed on human uterine cancer cells (26, 30). Although there are a number of publications concerning RCAS1 in cancers from the point of view as the 22-1-1 antigen, we consider that a pathophysiological role of EBAG9 in tumor immunology needs to be properly evaluated. The present manuscript may provide new insights into an EBAG9-mediated *in vivo* function in cancer progression.

We have previously reported that the immunoreactivity of EBAG9 was mainly observed in the cytoplasm of normal epithelial cells with a granular staining pattern, or particularly in perinuclear regions (3, 5). In carcinoma tissues, an intense staining of the cell surface could be also observed such as in prostate cancer or hepatocellular carcinoma. The expression of RCAS1 immunoreactivity recognized by antibodies against recombinant RCAS1 was localized to perinuclear structures, suggesting that the protein is predominantly distributed in the Golgi system (25). Given that EBAG9 is a Golgi-predominant protein that could be trafficking from the perinuclear regions to the cell surface membrane, it is likely that EBAG9 immunoreactivity could be observed in both cytoplasm and cell surface of cancerous tissues with the abundant expression of EBAG9. Notably, EBAG9 immunoreactivity in RCC with advanced stages such as sarcomatoid or metastatic tumors was cytoplasmic-predominant (Fig. 5C and 5D). Further studies using confocal or electron microscopic examination may elucidate the dynamic distribution of EBAG9.

As we showed that there are several types of cancer that intensely express EBAG9 and the expression levels of EBAG9 may relate to advanced tumor grades (3-6), it is likely that the tumor-promoting effect of EBAG9 is a general event in malignancies regardless of their estrogen dependency. We also observed the lack of association between sex and EBAG9 expression in human RCC in our clinicopathological study (Supplementary Table 1). Thus, EBAG9 could be a therapeutic target for various tumors constitutively expressing the molecule.

In summary, we demonstrate that EBAG9 is a tumor-promoting factor in both murine Renca RCC and human RCC. We propose that EBAG9 immunoreactivity is a new potential biomarker for prognosis of RCC and a treatment modality targeting EBAG9 will provide a novel therapeutic option for advanced RCC.

#### ACKNOWLEDGEMENTS

We thank T. Suzuki for her technical assistance.

**REFERENCES**

1. Watanabe T, Inoue S, Hiroi H, Orimo A, Kawashima H, Muramatsu M. Isolation of estrogen-responsive genes with a CpG island library. *Mol Cell Biol* 1998;18:442-9.
2. Tsuchiya F, Ikeda K, Tsutsumi O, et al. Molecular cloning and characterization of mouse EBAG9, homolog of a human cancer associated surface antigen: expression and regulation by estrogen. *Biochem Biophys Res Commun* 2001;284:2-10.
3. Suzuki T, Inoue S, Kawabata W, et al. EBAG9/RCAS1 in human breast carcinoma: a possible factor in endocrine-immune interactions. *Br J Cancer* 2001;85:1731-7.
4. Akahira JI, Aoki M, Suzuki T, et al. Expression of EBAG9/RCAS1 is associated with advanced disease in human epithelial ovarian cancer. *Br J Cancer* 2004;90:2197-202.
5. Takahashi S, Urano T, Tsuchiya F, et al. EBAG9/RCAS1 expression and its prognostic significance in prostatic cancer. *Int J Cancer* 2003;106:310-5.
6. Aoki T, Inoue S, Imamura H, et al. EBAG9/RCAS1 expression in hepatocellular carcinoma: correlation with tumour dedifferentiation and proliferation. *Eur J Cancer* 2003;39:1552-61.
7. Landis SH, Murray T, Bolden S, Wingo PA. Cancer statistics, 1999. *CA Cancer J Clin* 1999;49:8-31.
8. Moch H, Gasser T, Amin MB, Torhorst J, Sauter G, Mihatsch MJ. Prognostic utility of the recently recommended histologic classification and revised TNM staging system of renal cell carcinoma: a Swiss experience with 588 tumors. *Cancer* 2000;89:604-14.
9. Takeuchi T, Ueki T, Sasaki Y, et al. Th2-like response and antitumor effect of anti-interleukin-4 mAb in mice bearing renal cell carcinoma. *Cancer Immunol Immunother* 1997;43:375-81.
10. Nishimatsu H, Takeuchi T, Ueki T, et al. CD95 ligand expression enhances growth of murine renal cell carcinoma in vivo. *Cancer Immunol Immunother* 1999;48:56-61.
11. Gelb AB. Renal cell carcinoma: current prognostic factors. Union Internationale Contre le Cancer (UICC) and the American Joint Committee on Cancer (AJCC). *Cancer* 1997;80:981-6.
12. Dawson M. Initiation and maintenance of cultures. In: Bulter M, Dawson M editors. *Cell culture labfax*. Oxford: BIOS Scientific; 1992. p. 25-42.
13. Miyamoto T, Min W, Lillehoj HS. Lymphocyte proliferation response during *Eimeria tenella* infection assessed by a new, reliable, nonradioactive colorimetric assay. *Avian Dis* 2002;46:10-6.
14. Schumacher K, Haensch W, Roefzaad C, Schlag PM. Prognostic significance of activated CD8(+) T cell infiltrations within esophageal carcinomas. *Cancer Res* 2001;61:3932-6.
15. Shankaran V, Ikeda H, Bruce AT, et al. IFN $\gamma$  and lymphocytes prevent primary tumour development and shape tumour immunogenicity. *Nature* 2001;410:1107-11.
16. Pawelec G. Immunotherapy and immunoselection -- tumour escape as the final hurdle. *FEBS Lett* 2004;567:63-6.
17. Springer GF. Immunoreactive T and Tn epitopes in cancer diagnosis, prognosis, and immunotherapy. *J Mol Med* 1997;75:594-602.
18. Hakomori S. Glycosylation defining cancer malignancy: new wine in an old bottle. *Proc Natl Acad Sci U S A* 2002;99:10231-3.
19. Kudo D, Rayman P, Horton C, et al. Gangliosides expressed by the renal cell carcinoma cell

- line SK-RC-45 are involved in tumor-induced apoptosis of T cells. *Cancer Res* 2003;63:1676-83.
20. Thornton MV, Kudo D, Rayman P, et al. Degradation of NF-kappa B in T cells by gangliosides expressed on renal cell carcinomas. *J Immunol* 2004;172:3480-90.
  21. Ritter G, Livingston PO. Ganglioside antigens expressed by human cancer cells. *Semin Cancer Biol* 1991;2:401-9.
  22. Ito A, Levery SB, Saito S, Satoh M, Hakomori S. A novel ganglioside isolated from renal cell carcinoma. *J Biol Chem* 2001;276:16695-703.
  23. Caldwell S, Heitger A, Shen W, Liu Y, Taylor B, Ladisch S. Mechanisms of ganglioside inhibition of APC function. *J Immunol* 2003;171:1676-83.
  24. Manfredi MG, Lim S, Claffey KP, Seyfried TN. Gangliosides influence angiogenesis in an experimental mouse brain tumor. *Cancer Res* 1999;59:5392-7.
  25. Engelsberg A, Hermosilla R, Karsten U, Schulein R, Dorken B, Rehm A. The Golgi protein RCAS1 controls cell surface expression of tumor-associated O-linked glycan antigens. *J Biol Chem* 2003;278:22998-3007.
  26. Nakashima M, Sonoda K, Watanabe T. Inhibition of cell growth and induction of apoptotic cell death by the human tumor-associated antigen RCAS1. *Nat Med* 1999;5:938-42.
  27. Gnarr JR, Zhou S, Merrill MJ, et al. Post-transcriptional regulation of vascular endothelial growth factor mRNA by the product of the VHL tumor suppressor gene. *Proc Natl Acad Sci U S A* 1996;93:10589-94.
  28. Turner KJ, Moore JW, Jones A, et al. Expression of hypoxia-inducible factors in human renal cancer: relationship to angiogenesis and to the von Hippel-Lindau gene mutation. *Cancer Res* 2002;62:2957-61.
  29. Ohm JE, Gabrilovich DI, Sempowski GD, et al. VEGF inhibits T-cell development and may contribute to tumor-induced immune suppression. *Blood* 2003;101:4878-86.
  30. Sonoda K, Nakashima M, Kaku T, Kamura T, Nakano H, Watanabe T. A novel tumor-associated antigen expressed in human uterine and ovarian carcinomas. *Cancer* 1996;77:1501-9.

**FIGURE LEGENDS**

Fig. 1. Expression of EBAG9 siRNA suppresses tumor growth derived from murine renal cell carcinoma Renca cells in BALB/c mice. Subcutaneous primary Renca tumors were established by midflank injections of 10,000 tumor cells and intratumoral injections of either control scrambled siRNA or EBAG9 siRNA duplexes together with a transfection reagent GeneSilencer were performed twice a week in five mice per group when the initial tumor volumes reached 300 mm<sup>3</sup>. Mice were sacrificed after 4-weeks siRNA administration and tumors were homogenized for protein extraction. *A*, Western blot analysis of lysates from *in vitro* culture Renca cells and tumor samples expressing either control scrambled siRNA or EBAG9 siRNA. *B*, Representative mice after 4-weeks siRNA treatment. Upper panel, mouse treated with control scrambled siRNA; Lower panel, mouse treated with EBAG9 siRNA. *C*, Tumor volume in EBAG9 siRNA-treated mice (n = 5) is reduced compared with control mice (n = 5). \**P* < 0.05 at 4 weeks (EBAG9 siRNA *versus* scrambled siRNA).

Fig. 2. Overexpression of EBAG9 in Renca cells does not accelerate culture cell growth. *A*, RT-PCR analysis and Western blot analysis of Renca cells stably expressing human EBAG9 (Renca-EBAG9) or empty vector (Renca-vector). Upper panel, human EBAG9 mRNA is expressed in clones 3 and 4 of Renca-EBAG9 cells. Empty pcDNA3 vector was used as a negative control and pcDNA3 including EBAG9 cDNA as a positive control. Lower panel, EBAG9 protein is overexpressed in Renca-EBAG9 clones compared with Renca-vector clones or parental Renca cells. *B*, Doubling time of culture Renca cells. The numbers of cells in the exponential growth were counted every two days and doubling time was calculated according to a formula as described in Materials and Methods (n = 5 for each). *C*, Proliferative assay using WST-8 tetrasolium salt. Cells seeded into 96-well plates were transfected with control scrambled siRNA or EBAG9 siRNA duplexes (100 ng/well) and cell proliferation was evaluated on days 0, 2, and 4 (n = 3 for each). Absorbance at 450 nm (for formazan dye) was measured with absorbance at 620 nm for reference.

Fig. 3. Renca cells stably expressing EBAG9 develops large tumors in BALB/c mice. *A*, Representative mice 4 weeks after the inoculation of tumor cells. *B*, Volumes of tumors derived from Renca-EBAG9 cells are significantly larger compared with Renca-vector cells in BALB/c mice. Subcutaneous primary tumors were established by midflank injections of 10,000 tumor cells. \*\**P* < 0.01 at 4 weeks (Renca-EBAG9 *versus* Renca-vector). Renca-vector #1, n = 16; Renca-vector #2, n = 6; Renca-EBAG9 #3, n = 6; Renca-EBAG9 #4, n = 8. *C*, Poorer prognosis of mice inoculated with Renca-EBAG9 cells compared with mice with Renca-vector cells. Disease-specific survival on day 100: *P* = 0.0412 (Renca-EBAG9 *versus* Renca-vector). Renca-vector #1, n = 9; Renca-vector #2, n = 8; Renca-EBAG9 #3, n = 8; Renca-EBAG9 #4, n = 10.

Fig. 4. EBAG9 overexpression promotes renal subcapsular tumor growth by Renca cells in wild-type BALB/c mice. *A*, Representative tumors 25 days after the inoculation of tumor cells (10,000 cells). *B*, Volumes of Renca-EBAG9 tumors are larger than Renca-vector tumors in BALB/c mice, whereas no significant difference of tumor volumes between Renca-vector and Renca-EBAG9 in

BALB/c nude mice.  $**P < 0.0001$  on day 25 (Renca-EBAG9 *versus* Renca-vector). Renca-vector #1,  $n = 12$ ; Renca-vector #2,  $n = 11$ ; Renca-EBAG9 #3,  $n = 9$ ; Renca-EBAG9 #4,  $n = 9$ . *C*, Lysis of Renca-EBAG9 and Renca-vector cells by tumor-specific cytotoxic T lymphocytes (CTLs). Splenocytes from Renca-bearing mice were cultured with Renca cells at a ratio of 20:1 pulsed with interleukin-2 (1,000 U/ml) for 5 days. Lactate dehydrogenase release from cells with a damaged membrane was examined using CytoTox-ONE Reagent and fluorescence was measured with an excitation wave length of 560 nm and an emission wave length of 590 nm. *D*, Numbers of tumor infiltrating-lymphocytes positive for CD3, CD4, or CD8 immunostaining were microscopically examined in the high power field (HPF) of view at a magnification of 400X. BALB/c mouse spleen specimen was used as a positive control.  $*P < 0.05$  (Renca-EBAG9 *versus* Renca-vector).

Fig. 5. EBAG9 immunostaining in human kidney and renal cell carcinoma specimens. *A*, Normal kidney (IR score 0). EBAG9 is weakly expressed in the mesangial cells (arrow heads). *B*, Clear cell carcinoma (IR score 1+). EBAG9 is immunostained predominantly on the cell membrane in carcinous regions. *C*, Spindle cell carcinoma (IR score 3+). Intense immunostaining of EBAG9 is observed in the cytoplasm of sarcomatoid carcinous regions. *D*, Lung metastatic tumors (IR score 3+). Intense immunoreactivity of EBAG9 is observed in metastatic tumors with high IR scores. Bars represent 50  $\mu\text{m}$ .

Fig. 6. Association of immunocytochemical staining for EBAG9 with disease-specific survival of 78 RCC patients. Five-year disease-specific survival of the patients with high EBAG9 immunoreactivity (IR score 3+,  $n = 19$ ) was significantly worse than the patients with IR scores 0-2+ ( $n = 59$ ) (55% *versus* 91%,  $P = 0.0007$ , by log-rank test).

Supplementary Table 1 *Association between EBAG9 immunoreactivity and clinicopathological parameters in human RCC patients*

Variable	n	EBAG9 immunoreactivity		P Value <sup>a</sup>
		Negative	Positive <sup>b</sup>	
Patients	78	10	68	
Lymph node status				> 0.9999
Positive	6	0	6	
Negative	72	10	62	
Metastatic status				0.5857
Positive	7	0	7	
Negative	71	10	61	
Age		57.5 ± 8.1 <sup>c</sup> 54.1 ± 11.7		0.3849
Sex				0.3735
Male	64	7	57	
Female	14	3	11	
Infiltration				0.3263
α	43	7	36	
β, γ	35	3	32	
Grade				0.0606
1	24	6	18	
2, 3	54	4	50	
Histological type				0.0126*
Clear cell	51	10	41	
Others	27	0	27	
Vascular infiltration				0.0109*
Positive	29	0	29	
Negative	49	10	39	
Pathological stage				0.0017*
T1	43	10	33	
≥T2	35	0	35	

<sup>a</sup>Evaluated by the student-t test/ Fisher's exact probability test.

<sup>b</sup>Defined positive if >5% of cells were stained.

<sup>c</sup>Mean ± standard deviation.

\**P* < 0.05.

Supplementary Table 2 *Correlation between 5-year cancer-specific survival and clinicopathological parameters in RCC patients*

Variable	n	Survival (%)	P Value <sup>a</sup>
Patients	78		
Age			0.5828
<60	49	85.5	
≥60	29	77.4	
Grade			0.0254 <sup>*</sup>
1	24	95.7	
2, 3	54	76.8	
Histological type			0.0205 <sup>*</sup>
Clear cell	51	89.8	
Others	27	70.4	
EBAG9 immunoreactivity			0.0007 <sup>*</sup>
Low (0, 1+ & 2+)	59	91.2	
High (3+)	19	55	
Vascular infiltration			0.0003 <sup>*</sup>
Positive	29	62.4	
Negative	49	93.9	
Lymph node status			0.0002 <sup>*</sup>
Positive	6	33.3	
Negative	72	86.9	
Infiltration			< 0.0001 <sup>*</sup>
α	41	97.5	
β, γ	37	65.5	
Pathological stage			< 0.0001 <sup>*</sup>
T1	43	97.6	
≥T2	35	63.6	
Metastatic status			< 0.0001 <sup>*</sup>
Positive	7	0	
Negative	71	91.2	

<sup>a</sup>Determined by the log-rank test.

<sup>\*</sup>*P* < 0.05.

Supplementary Table 3 *Multivariate analysis of prognostic factors in Cox regression hazard model*

Variable	Relative risk	95% confidence interval	P value
Grade (2, 3/ 1)	1.081	0.099 - 11.835	0.9490
Vascular infiltration (positive/ negative)	0.938	0.213 - 4.139	0.9326
Pathological stage ( $\geq$ T2/ T1)	8.702	0.973 - 77.831	0.5290
Lymph node status (positive/ negative)	0.385	0.087 - 1.700	0.2077
Infiltration ( $\beta$ , $\gamma$ / $\alpha$ )	4.342	0.485 - 38.883	0.1892
Histological type (others/ clear cell)	3.874	0.817 - 18.365	0.0880
EBAG9 immunoreactivity (3+/ 0,1+, and 2+)	5.092	1.010 - 25.662	0.0485*
Metastatic status (positive/ negative)	42.534	7.138 - 253.469	< 0.001*

\* $P < 0.05$

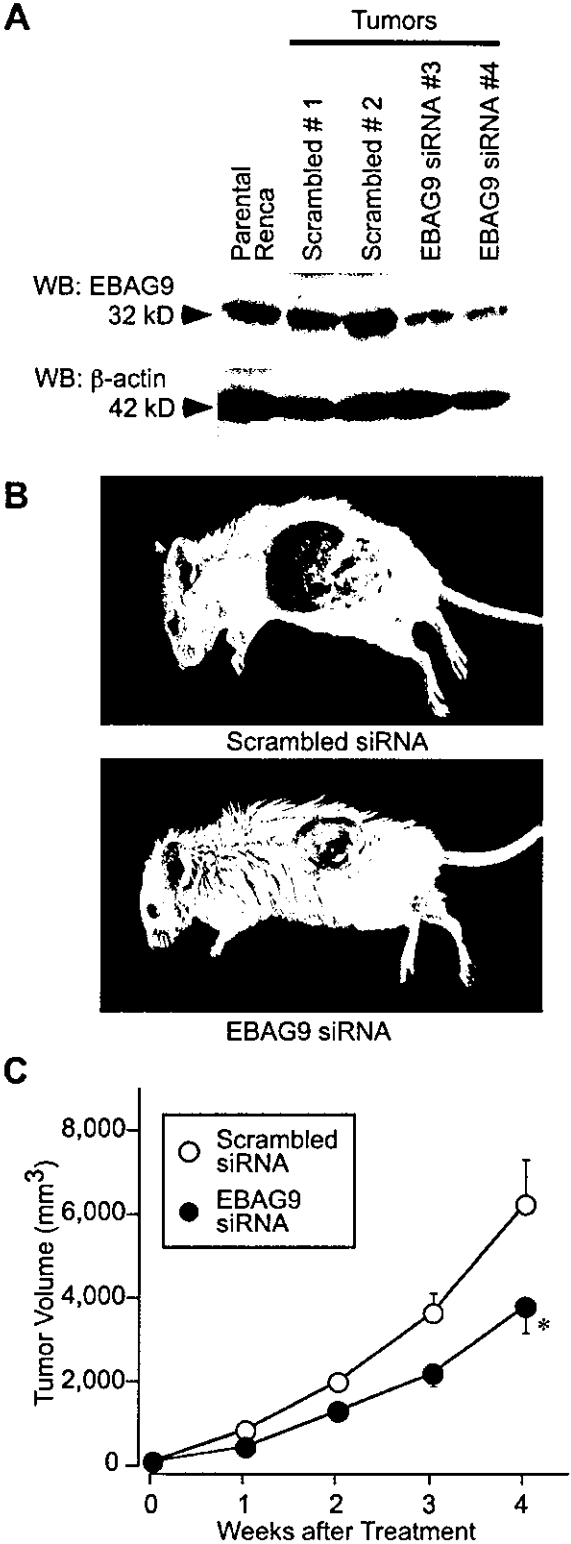


Fig. 1

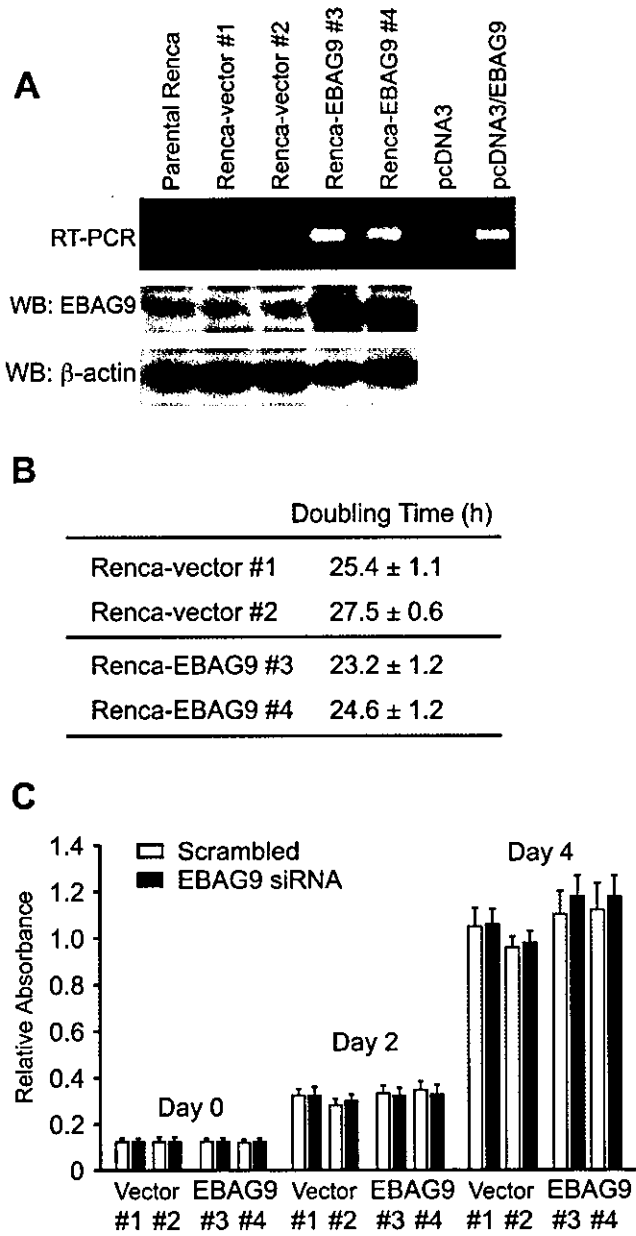


Fig. 2

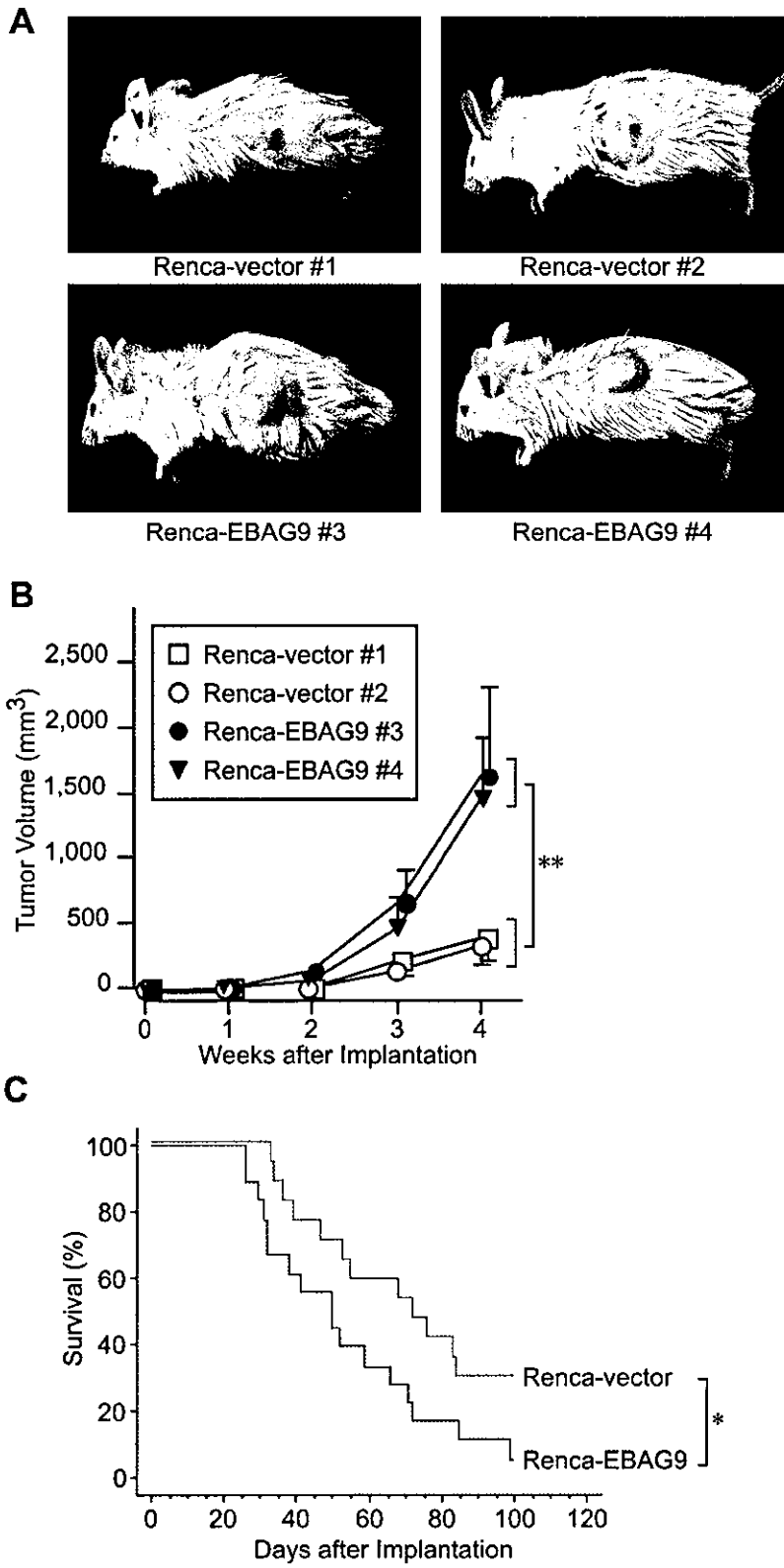


Fig. 3

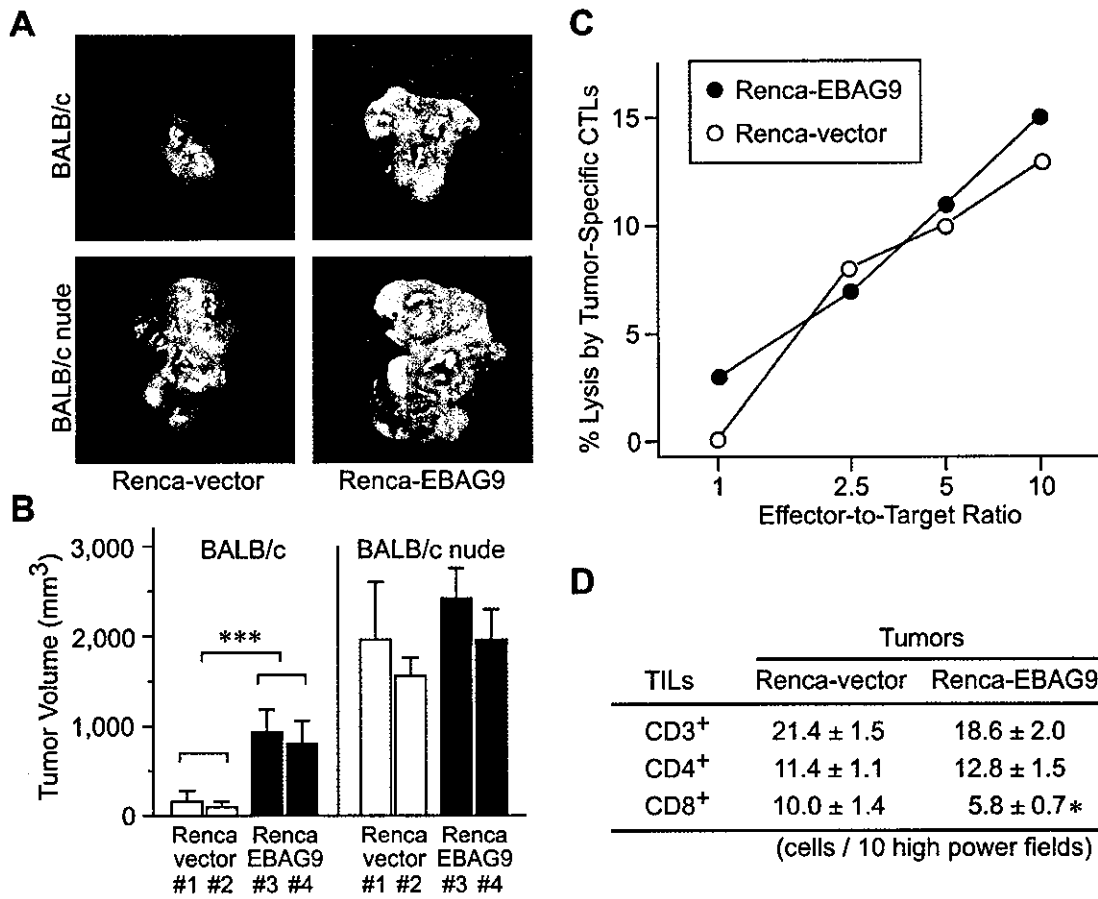


Fig. 4

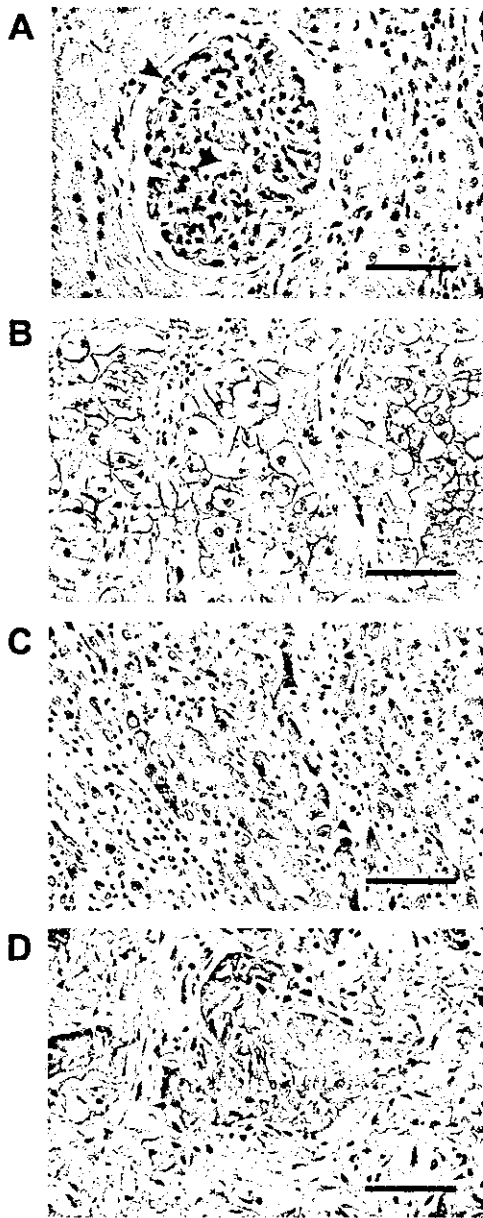


Fig. 5

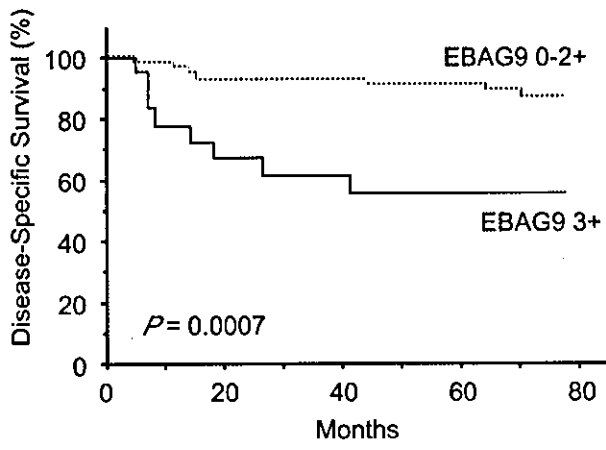


Fig. 6

## Association of a single nucleotide polymorphism in the lipoxygenase *ALOX15* 5'-flanking region (-5229G/A) with bone mineral density

Tomohiko Urano<sup>1)</sup>, Masataka Shiraki<sup>2)</sup>, Masayo Fujita<sup>1, 3)</sup>, Takayuki Hosoi<sup>4)</sup>, Hajime Orimo<sup>5)</sup>, Yasuyoshi Ouchi<sup>1)</sup>, Satoshi Inoue<sup>1, 3)</sup>

1) Department of Geriatric Medicine, Graduate School of Medicine, University of Tokyo, 7-3-1 Hongo, Bunkyo-ku, Tokyo, 113-8655, Japan, 2) Research Institute and Practice for Involuntal Diseases, 1609 Meisei, Misato-mura, Minami-Azumi-gun, Nagano, 399-8101, Japan, 3) Research Center for Genomic Medicine, Saitama Medical School, 1397-1, Yamane, Hidaka-shi, Saitama, 350-1241 Japan, 4) Tokyo Metropolitan Geriatric Hospital, 35-2 Sakae-cho, Itabashi-ku, Tokyo, 173-0015, Japan, 5) Health Science University, 7187 Kodachi, Kawaguchiko-machi, Minami-Tsuru-gun, Yamanashi, 401-0380, Japan

Offprint requests to: S. Inoue (Email: [INOUE-GER@h.u-tokyo.ac.jp](mailto:INOUE-GER@h.u-tokyo.ac.jp))

Short title: Association of an SNP in *ALOX15* gene with BMD

### Abstract

The 12/15-lipoxygenase gene *Alox15* has been identified as a susceptibility gene for bone mineral density in mice through combined genetic and genomic analyses. Here, we studied the association between bone mineral density and an *ALOX15* gene single nucleotide polymorphism to assess the potential involvement of the human *ALOX15* gene in the postmenopausal osteoporosis. Specifically we examined the association between a single nucleotide polymorphism at -5299G/A in the *ALOX15* 5'-flanking region with BMD in 319 postmenopausal Japanese women ( $66.7 \pm 8.9$  years, mean  $\pm$  SD). We found that subjects bearing at least one variant A allele (GA + AA; n=273) had significantly lower Z scores for lumbar spine and total body bone mineral density than did subjects with no A allele (GG; n=46) (lumbar spine,  $-0.25 \pm 1.34$  versus  $0.48 \pm 1.70$ ;  $p = 0.0014$ ; total body,  $0.25 \pm 1.01$  versus  $0.62 \pm 1.11$ ;  $p = 0.048$ ). These findings suggest that the *ALOX15* gene is one of the genetic determinants of BMD in postmenopausal women. Accordingly, this polymorphism could be useful as a genetic marker for predicting the risk of osteoporosis.

**Key words** adipogenesis, *ALOX15*, PPAR $\gamma$ , osteoporosis, bone mineral density, polymorphism

## Introduction

Osteoporosis is characterized by low bone mineral density (BMD), increased bone fragility, and consequently increased risk of fracture [1]. Studies of twins and siblings have shown that BMD is under genetic control, with estimates of heritability ranging from 50% to 90% [2,3]. BMD is regulated by interaction of multiple environmental and genetic factors, each having modest effects on bone mass and bone turnover [4,5]. Polymorphisms of several genes have been investigated to clarify the determinants of BMD [6,7]. These genes of which polymorphisms were associated with BMD include those implicated in bone formation by regulation of osteoblast growth and function, such as *vitamin D receptor* gene [8], *transforming growth factor beta1 (TGFB1)* gene, *collagen type Ia1 (COL1A1)* gene [9], *peroxisome proliferator activated receptor- $\gamma$  (PPAR $\gamma$ )* gene [10] and *low-density lipoprotein receptor-related protein 5 (LRP5)* gene [11]. Identification of candidate genes that affect bone mass will be useful for early detection of individuals who are at risk of osteoporosis and early institution of preventive measures.

The decrease in bone volume associated with osteoporosis is accompanied by an increase in marrow adipose tissues [12, 13]. Indeed, an increase in marrow adipocytes is observed in several conditions that lead to bone loss, such as ovariectomy [14], immobilization [15], and treatment with glucocorticoids [16]. Recent studies have identified rodent quantitative trait locus associated with increased BMD in the mouse gene encoding 12/15-lipoxygenase [17], the enzyme that converts linoleic acid and arachidonic acid into endogenous ligands for the PPAR $\gamma$  [18-20]. Activation of this pathway in marrow-derived mesenchymal progenitors stimulates adipogenesis and inhibits osteoblastogenesis [21, 22]. Mice that are deficient in this gene or have been treated with 12/15-lipoxygenase inhibitors demonstrate increased bone mass as compared with controls [17]. These findings suggest that genetic variants of the 12/15-lipoxygenase encoding gene may affect the BMD in humans as well as mice. The mouse 12/15-lipoxygenase enzyme corresponds to at least three lipoxygenases in humans. 15-lipoxygenase has two isoenzymes: type 1 (human *ALOX15*, encoded by a gene at chromosome 17p13.3) and type 2 (human *ALOX15B*, encoded by a separate gene at 17p13.1). 12-lipoxygenase (human *ALOX12*, encoded by a gene at chromosome 17p13.1) is predominantly expressed in platelets and macrophages and is distinct from 15-lipoxygenase [23]. In the present study, we examined the possibility that there is an association between a polymorphism in the human *ALOX15* gene and BMD in Japanese women to investigate possible contribution of the lipoxygenase in the bone metabolism.

## **Materials and methods**

### ***Subjects***

We analyzed genotypes in DNA samples from 319 healthy postmenopausal Japanese women ( $66.7 \pm 8.9$  years, mean  $\pm$  SD). We excluded women having endocrine disorders such as hyperthyroidism, hyperparathyroidism, diabetes mellitus, liver disease, and renal disease; those who used medications known to affect bone metabolism (e.g., corticosteroids, anticonvulsants, and heparin); and those with an unusual gynecologic history. All subjects were unrelated volunteers. Each subject was provided informed consent before entering the study.

### ***Measurement of bone mineral density and biochemical markers***

We measured the lumbar spine BMD and total body BMD of participants by dual-energy X-ray absorptiometry using the fast-scan mode (DPX-L; Lunar, Madison, WI). The BMD data were recorded as Z scores, as the deviation from the weight-adjusted average BMD for each year of age, based on data from 20,000 Japanese women. We also measured subjects' serum concentrations of alkaline phosphatase (ALP), intact osteocalcin (I-OC), intact parathyroid hormone (PTH), calcitonin,  $1,25(\text{OH})_2\text{D}_3$ , total cholesterol (TC) and triglyceride (TG). We also measured urinary ratios of deoxypyridinoline (DPD) to creatinine using the HPLC method.

### ***Determination of a single nucleotide polymorphism in the ALOX15 gene***

We extracted a polymorphic variation of the putative *ALOX15* gene promoter/enhancer region from the Assays-on-Demand™ SNP Genotyping Products database (Applied Biosystems, Foster City, CA) and, according to its localization on the gene, denoted it -5299 G>A. We determined the -5299G/A polymorphism of the *ALOX15* gene using the TaqMan (Applied Biosystems) polymerase chain reaction (PCR) method [24]. To determine the *ALOX15* SNP we used Assays-on-Demand SNP Genotyping Products C\_926671\_10 (Applied BioSystems), which contains sequence-specific forward and reverse primers and two TaqMan MGB probes for detecting alleles. During the PCR cycle, two TaqMan probes competitively hybridize to a specific sequence of the target DNA and the reporter dye is separated from the quencher dye, resulting in an increase in fluorescence of the reporter dye. The fluorescence levels of the PCR products were measured with the ABI PRISM 7000 (Applied Biosystems), resulting in clear identification of three genotypes of the SNP.

### ***Statistical analysis***

We divided subjects into those having one or two chromosomes of the major A-allele and those with only the minor G-allele encoded at the same locus. Comparisons of Z scores and biochemical markers between these two groups were subjected to

statistical analysis (Student's *t*-test; StatView-J 4.5). A *P*-value of less than 0.05 was considered statistically significant.

## Results

### *Association of ALOX15 Gene Polymorphism With Bone Mineral Density*

Among our 319 subjects, 46 were GG homozygotes, 155 were GA heterozygotes, and 118 were AA homozygotes. Allelic frequencies were 0.613 for the A allele and 0.387 for the G allele in this population. The allelic frequencies of this SNP in the present study were in Hardy-Weinberg equilibrium.

We compared the 273 subjects bearing at least one chromosome with the A allele (genotype GA + AA) and the 46 subjects having no A allele (GG) with respect to their Z scores for lumbar spine and total body BMD. Those with the A allele had significantly lower Z scores for lumbar spine BMD ( $-0.25 \pm 1.34$  versus  $0.48 \pm 1.70$ ;  $p = 0.0014$ ) (Fig. 1A) and total body BMD ( $0.25 \pm 1.01$  versus  $0.62 \pm 1.11$ ;  $p = 0.048$ ) (Fig. 1B). As shown in Table 1, the background and biochemical data did not significantly differ between these groups.

## Discussion

Various regulating elements have been identified within the *ALOX15* 5'-flanking promoter/enhancer region, including a site for binding with Sp1 [25], AP1 [25], and GATA [26], as well as sites for methylation [27] and acetylation [28, 29] and a Stat6 response element [29], suggesting that 15-lipoxygenase expression is directly regulated through transcription regulation. In the present study, we observed a significant association between BMD and a G/A SNP at the -5299 site in the *ALOX15* 5'-flanking region. This is the first report to our knowledge that a common SNP in the *ALOX15* gene affects on BMD. One possible explanation for this effect is that this 5' -flanking region polymorphism may be involved in the newly defined transcriptional regulating element of the *ALOX15* promoter/enhancer. Alternatively, the 5'-flanking region polymorphism may have a linkage with another base of the *ALOX15* promoter/enhancer that may control transcription of the *ALOX15* gene. It is also possible that this SNP may be linked with mutation of the *ALOX15* exons or another unidentified gene adjacent to the *ALOX15* locus, which affect on the bone mass.

Although there are three lipoxygenases in humans, *ALOX15*, *ALOX15B*, and *ALOX12*, that correspond to 12/15-lipoxygenase in mice [23], we know little of their

roles in human bone metabolism. Our results suggest that the 15-lipoxygenase type1, the *ALOX15*, may have a specific function in the regulation of bone mass in human. It should be required to determine how signals from 15-lipoxygenase can be transduced to the regulation of the bone metabolism.

Three major cellular events are involved in senile osteoporosis; they are declining levels of osteogenesis, increasing numbers of apoptotic osteoblasts and osteocytes, and increasing levels of bone marrow adipogenesis [30-32]. The bone marrow adipogenesis that occurs with aging may be due to alterations in cell differentiation, in part by PPAR $\gamma$  activation [33-35] and increasing lipid oxidation [36]. Previous reports demonstrated that 12/15-lipoxygenases are involved in this system [17, 18, 37, 38], suggesting that 12/15-lipoxygenase may increase with aging in progenitor cells and activate adipogenesis. It has been also shown that 12/15-lipoxygenase is increased in Alzheimer's disease, which is the most common neurodegenerative disorder of the elderly [39]. Therefore, it is tempting to speculate that 12/15-lipoxygenase is increased associated with aging and senile osteoporosis. To test this hypothesis, measurement of 12/15-lipoxygenase activity and association study between BMD and the *ALOX15* gene SNP in older subjects would be desired.

In conclusion, our finding suggests that the *ALOX15* gene may be a genetic determinant of BMD in postmenopausal women. Examining the variation in the *ALOX15* gene will hopefully enable us to elucidate one of the mechanisms of involutional osteoporosis. Furthermore, the variation may be a potential genetic susceptibility factor that need to be further evaluated with regard to the risk of other diseases in which 15-lipoxygenase have been clearly implicated, including atherosclerosis [40], asthma [41], cancer [42] and glomerulonephritis [43].

#### Acknowledgments

This work was partly supported by grants from the Japanese Ministry of Health, Labor and Welfare and the Japanese Ministry of Education, Culture, Sports, Science and Technology. We thank Ms. E. Sekine, C. Onodera, and M. Kumasaka for expert technical assistances.

#### References

1. Kanis JA, Melton LJ 3rd, Christiansen C, Johnston CC, Khaltsev N (1994) The diagnosis of osteoporosis. *J Bone Miner Res* 9:1137-1141
2. Flicker L, Hopper JL, Rodgers L, Kaymakci B, Green RM, Wark JD (1995) Bone density determinants in elderly women: a twin study. *J Bone Miner Res* 10:1607-